Journal of Biomolecular NMR, 8 (1996) 331–344
ESCOM

J-Bio NMR 375

The secondary structure of a pyrimidine-guanine sequence-specific ribonuclease possessing cytotoxic activity from the oocytes of *Rana catesbeiana*

Chinpan Chen[a], Kellie Hom[a,*], Rong-Fong Huang[a], Ping-Jung Chou[a], You-Di Liao[b] and Tai-huang Huang[a,**]

Divisions of [a]Structural Biology and [b]Cancer Research, Institute of Biomedical Sciences, Academia Sinica, Nankang, Taipei 11529, Taiwan, Republic of China

Received 5 February 1996
Accepted 16 May 1996

Keywords: RC-RNase; Cytotoxicity; Sialic acid

Summary

RC-RNase is a pyrimidine-guanine sequence-specific ribonuclease and a sialic-acid-binding lectin purified from *Rana catesbeiana* (bullfrog) oocytes. This 111-amino acid protein exhibits cytotoxicity toward several tumor cell lines. In this paper we report the assignments of proton NMR resonances and the identification of the secondary structure deduced from NOE constraints, chemical shift index, $^3J_{NH\alpha}$ and amide proton exchange rates. The protein was directly isolated from bullfrog oocytes; we were able to assign all but five of the amino acid backbone protons of the unlabeled protein by analyzing a large set of two-dimensional proton NMR spectra obtained at several temperatures and pH conditions. Our results indicate that the structure of RC-RNase is dominated by the presence of two triple-stranded antiparallel β-sheets and three α-helices, similar to those of the pyrimidine family ribonucleases. Two sets of resonances were observed for 11 amide protons and 8 α-protons located in the loop-1 region, an α2 helix, and three β-strands (β1, β3 and β4), suggesting the presence of nonlocalized multiple conformations for RC-RNase.

Introduction

RC-RNase is a pyrimidine-guanine sequence-specific ribonuclease isolated from *Rana catesbeiana* (bullfrog) oocytes (Liao, 1992). Compared to single-stranded RNA, double-stranded RNA is relatively resistant to RC-RNase. The activity of RC-RNase in the oocyte has been found to be regulated by both inhibitor binding and compartmentation (Liao and Wang, 1994), with 99% of the protein found in the yolk granules and the remaining 1% in the cytosol (Liao et al., 1996). Partial sequencing of RC-RNase indicated that it was highly homologous to SBL-C, a sialic-acid-binding lectin isolated from *Rana catesbeiana* oocyte (Kawauchi et al., 1975; Titani et al., 1987). SBL-C is known to preferentially agglutinate cells from a large variety of human and animal tumor cell lines, but not red blood cells, lymphocytes, fibroblasts or neuramidase-treated tumor cells (Sakakibara et al., 1979; Okabe et al., 1991; Nitta et al., 1994); it also displays a specific binding to sialyl glycoprotein (Sakakibara et al., 1979), preferably the clustered sialyl oligosaccharides O-glycosidically linked to the peptide backbone at the surface of tumor cells. It is now known (vide infra), from complete sequencing and mass spectrometry, that RC-RNase and SBL-C are identical in sequence, and we refer to this protein as RC-RNase. Binding of this protein inhibits the growth of tumor cells such as P388 and L1210 leukemia cells in vitro, and is effective for in vivo killing of Sar-

*Present address: Department of Pharmaceutical Chemistry, University of California, San Francisco, CA 94143-0446, U.S.A.
**To whom correspondence should be addressed.

Abbreviations: DQF-COSY, double-quantum-filtered correlation spectroscopy; DTT, dithiothreitol; NOE, nuclear Overhauser enhancement; NOESY, nuclear Overhauser enhancement spectroscopy; PE-1, N-terminal pyroglutamate; RC-RNase, ribonuclease from the oocyte of *Rana catesbeiana*; TOCSY, total correlation spectroscopy; TPPI, time-proportional phase incrementation; TSP, sodium 3-trimethylsilylpropionate-2,2,3,3-d_4.

TABLE 1
^{1}H CHEMICAL SHIFTS FOR RC-RNase[a]

Residue	Chemical shift (ppm)				
	NH	$C^{\alpha}H$	$C^{\beta}H$	$C^{\gamma}H$	Others
PE-1[b]		3.89			
Asn[2]	8.04	4.65	3.31, 3.21		$N^{\delta}H_2$ 7.82, 7.12
Trp[3]	9.36	5.54	3.17, 3.04		$N^{\varepsilon}H$ 10.41; 2H 7.14; 4H 8.42; 5H 6.87; 6H 7.37; 7H 7.46
Ala[4]	8.72	3.80	1.40		
Thr[5]	8.55	4.00	3.90	1.31	
Phe[6]	8.83	4.34	3.62, 3.20		$C_{2,6}H$ 7.20; $C_{3,5}H$ 7.01; C_4H 6.83
Gln[7]	8.39	3.55	1.30, 1.67	1.85, 1.85	
Gln[8]	7.41	3.91	2.20, 2.03	2.43, 2.43	$N^{\varepsilon}H_2$ 7.28, 6.64
Lys[9]	8.22	3.96	1.44, 1.00	0.85, 0.85	$C^{\delta}H_2$ 1.37, 1.37; $C^{\varepsilon}H_2$ 2.02, 2.02
His[10]	7.90	4.65	2.75, 2.19		$C^{\varepsilon 1}H$ 8.52; $C^{\delta 2}H$ 6.59
Ile[11]	8.50	5.02	2.03	1.72, 1.13	$C^{\gamma}H_3$ 0.95; $C^{\delta}H_3$ 0.95
Ile[12]	8.72	4.81	1.83	1.35, 1.35	$C^{\gamma}H_3$ 0.86; $C^{\delta}H_3$ 0.86
Asn[13]	8.19	4.90	2.88, 2.88		$N^{\delta}H_2$ 7.32, 6.76
Thr[14]	7.14	4.84	4.17	1.11	
Pro[15]		4.35	1.73, 1.73	2.37, 2.05	$C^{\delta}H_2$ 3.72, 3.58
Ile[16]	7.70	4.01	1.76	1.32, 1.03	$C^{\gamma}H_3$ 0.71; $C^{\delta}H_3$ 0.62
Ile[17]	7.72 (7.74)	4.13	1.42		$C^{\gamma}H_3$ 0.71; $C^{\delta}H_3$ 0.49
Asn[18]	8.26	4.88	3.07, 2.62		$N^{\delta}H_2$ 7.54, 7.04
Cys[19]	9.51	4.06	2.81, 2.43		
Asn[20]	8.19	4.48	2.98, 2.98		$N^{\delta}H_2$ 7.40, 6.90
Thr[21]	7.39	4.30	4.18	1.23	
Ile[22]	7.96 (7.99)	3.99	1.53		0.64
Met[23]	7.19	4.56	1.39, 0.51	2.17, 1.70	
Asp[24]	7.16	4.94	3.12, 2.63		
Asn[25]	8.03	4.69	2.85, 2.66		$N^{\delta}H_2$ 8.15, 6.85
Asn[26]	8.94	4.36	2.87, 2.82		$N^{\delta}H_2$ 7.45, 6.81
Ile[27]	8.15	4.04	1.53		$C^{\gamma}H_3$ 0.55; $C^{\delta}H_3$ 0.28
Tyr[28]	7.80	4.76	3.51, 3.13		$C_{2,6}H$ 6.96; $C_{3,5}H$ 6.54
Ile[29]	7.35	4.51	2.14		0.69
Val[30]	8.53	4.40	2.04	1.01, 1.01	
Gly[31]	9.36	3.93, 3.93			
Gly[32]	8.34	4.20, 3.56			
Gln[33]	7.64	4.85	2.09, 1.97	2.35, 2.35	$N^{\varepsilon}H_2$ 7.50, 6.80
Cys[34]	8.43	3.83	2.40, 1.08		
Lys[35]	8.38	4.25	1.66, 1.66	1.00, 1.00	$C^{\delta}H_2$ 1.14, 1.14
Arg[36]	9.02	3.87	2.08, 1.90	1.79, 1.65	$C^{\delta}H_2$ 3.38, 3.23; $N^{\varepsilon}H$ 7.37
Val[37]	7.71 (7.65)	5.41 (5.34)	2.01	0.96, 0.91	
Asn[38]	8.41	4.84	2.21, 1.92		$N^{\delta}H_2$ 7.87, 7.31
Thr[39]	8.80	4.46	4.41	0.81	
Phe[40]	9.38	4.77	3.07, 2.71		$C_{2,6}H$ 7.08; $C_{3,5}H$ 6.93; C_4H 7.03
Ile[41]	9.36	4.32	1.74	0.78, 0.78	$C^{\gamma}H_3$ 0.70; $C^{\delta}H_3$ 0.58
Ile[42]	8.68 (8.66)	4.89 (4.87)	1.96	1.27, 1.27	$C^{\gamma}H_3$ 0.74; $C^{\delta}H_3$ 0.62
Ser[43]	8.10	4.65	4.23, 3.26		
Ser[44]	8.41	4.73	4.27, 4.10		
Ala[45]	9.34	4.32	1.77		
Thr[46]	8.28	4.01	4.24	1.38	
Thr[47]	7.47	4.08	4.41	1.42	
Val[48]	7.47	3.83	2.40	1.09, 1.06	
Lys[49]	8.56	3.07	1.80, 1.68	1.03, 0.60	$C^{\delta}H_2$ 1.32, 1.32; $C^{\varepsilon}H_2$ 2.59, 2.28
Ala[50]	7.28	4.05	1.54		
Ile[51]	7.68	3.77	1.70	1.00, 1.00	$C^{\gamma}H_3$ 0.78; $C^{\delta}H_3$ 0.78
Cys[52]	7.27	4.72	2.85, 2.01		
Thr[53]	7.34	3.75	4.01	1.20	
Gly[54]	9.24	4.08, 3.54			
Val[55]	8.05	4.04	1.87	0.79, 0.79	
Ile[56]	8.14	3.85	1.97	1.47, 1.47	$C^{\gamma}H_3$ 0.98; $C^{\delta}H_3$ 0.77
Asn[57]	8.49	5.30	2.88, 2.83		$N^{\delta}H_2$ 7.46, 6.77
Met[58]	8.15	4.50	2.55, 2.55	2.71, 1.71	
Asn[59]	8.51	5.52	2.68, 2.37		$N^{\delta}H_2$ 7.41, 6.44

TABLE I
(continued)

Residue	Chemical shift (ppm)				
	NH	$C^{\alpha}H$	$C^{\beta}H$	$C^{\gamma}H$	Others
Val^{60}	9.13	4.20	1.82	0.90, 0.84	
Leu^{61}	8.20	4.83	1.73, 1.35	1.08	0.70, 0.50
Ser^{62}	9.69	4.47	4.96, 4.33		OH 6.13
Thr^{63}	7.52	4.60	3.95	0.98	
Thr^{64}	8.81	4.34	4.34	1.34	
Arg^{65}	8.41	3.71	1.34, 1.34	1.07, 0.18	$C^{\delta}H_2$ 2.86, 2.75; $N^{\varepsilon}H$ 6.84
Phe^{66}	8.54 (8.57)	4.54 (4.57)	3.03, 2.70		$C_{2,6}H$ 7.45; $C_{3,5}H$ 7.36; C_4H 7.45
Gln^{67}	9.20 (9.34)	4.57 (4.51)	2.24, 2.15	2.47, 2.40	$N^{\varepsilon}H_2$ 7.36, 6.87
Leu^{68}	8.96 (8.99)	5.58 (5.57)	1.85, 1.85	1.99	1.28, 0.82
Asn^{69}	9.00 (8.96)	5.23 (5.18)	2.82, 2.46		$N^{\delta}H_2$ 6.87, 6.54
Thr^{70}	9.16	4.98	3.92	1.00	
Cys^{71}	8.80	5.76	2.89, 2.70		
Thr^{72}	9.27	5.12	3.89	1.22	
Arg^{73}	9.62	3.52	1.75, 1.18		
Thr^{74}	9.04	4.31	4.12	1.18	
Ser^{75}	7.14	4.43	3.66, 3.63		
Ile^{76}	8.15	4.04	1.71		$C^{\gamma}H_3$ 0.86; $C^{\delta}H_3$ 0.68
Thr^{77}	7.43	4.84	3.33	0.97	
Pro^{78}			1.77, 1.65	1.96, 1.89	$C^{\delta}H_2$ 3.84, 3.67
Arg^{79}					
Pro^{80}					
Cys^{81}	8.43	3.83	2.21, 1.93		
Pro^{82}		4.84	1.83, 1.83	1.47, 1.47	$C^{\delta}H_2$ 3.25, 3.24
Tyr^{83}	8.94	5.17	2.60, 2.52		$C_{2,6}H$ 7.23 (6.52); $C_{3,5}H$ 6.75 (6.60)
Ser^{84}	9.33	4.83	3.97, 3.79		
Ser^{85}	8.41	5.55	4.04, 3.68		
Arg^{86}	8.50 (8.49)	4.82 (4.81)	1.84, 1.84	1.72, 1.47	$C^{\delta}H_2$ 3.26, 3.25; $N^{\varepsilon}H$ 7.16
Thr^{87}	8.78 (8.80)	5.40 (5.30)	4.30 (4.32)	1.25	
Glu^{88}	8.48 (8.44)	4.71 (4.75)	1.93, 1.93	2.20, 2.12	
Thr^{89}	8.51	5.51	3.89	0.92	
Asn^{90}	8.50	5.85	2.57, 2.54		$N^{\delta}H_2$ 7.25, 6.61
Tyr^{91}	9.20	4.58	2.87, 2.51		$C_{2,6}H$ 7.06; $C_{3,5}H$ 6.70
Ile^{92}	8.82	4.98	2.35	1.12, 0.73	$C^{\gamma}H_3$ 0.53; $C^{\delta}H_3$ 0.32
Cys^{93}	8.70	5.73	3.09, 2.06		
Val^{94}	8.85	4.79	1.91	0.73, 0.73	
Lys^{95}	8.31	4.78	1.92, 1.88	1.03, 1.03	$C^{\delta}H_2$ 1.55, 1.55
Cys^{96}	8.70	5.25	2.94, 2.53		
Glu^{97}	9.11	5.07	2.05, 1.82	2.38, 2.27	
Asn^{98}	10.43	4.38	3.23, 2.88		$N^{\delta}H_2$ 7.70, 6.95
Gln^{99}	8.04	4.13	1.98, 1.74	2.17, 2.03	$N^{\varepsilon}H_2$ 7.60, 6.87
Tyr^{100}	7.66	4.56	2.67, 2.46		$C_{2,6}H$ 6.60; $C_{3,5}H$ 6.32
Pro^{101}		4.64	2.23, 2.23	1.90, 1.90	$C^{\delta}H_2$ 3.84, 3.67
Val^{102}	8.50	4.59	1.80	0.97, 0.73	
His^{103}	7.30	5.66	3.23, 3.17		$C^{\varepsilon 1}H$ 8.68; $C^{\delta 2}H$ 7.17
Phe^{104}	10.27	4.30	3.10, 1.66		$C_{2,6}H$ 6.81; $C_{3,5}H$ 7.01
Ala^{105}	8.28	4.57	0.98		
Gly^{106}	6.64	4.29, 4.05			
Ile^{107}	8.51	4.60			
Gly^{108}	9.12	4.54, 3.49			
Arg^{109}	7.26	4.48	1.95, 1.75	1.60, 1.33	$C^{\delta}H_2$ 3.19, 3.16; $N^{\varepsilon}H$ 7.04
Cys^{110}	8.87	4.92	3.37, 2.89		
Pro^{111}					

[a] In 90%/10% H_2O/D_2O at 310 K, pH 3.5, taking the TSP resonance (0.00 ppm) as a reference. The chemical shifts of second conformers are parenthesized.

[b] PE-1 represents N-terminal pyroglutamate.

coma 180, Ehrlich, and Mep II ascites cells (Nitta et al., 1994). There is evidence that the anti-proliferative activity of RC-RNase on tumor cells might be effected by the following events: (i) the binding of RC-RNase to sialoglyco-

conjugated lectin receptor on the tumor cell surface; (ii) the endocytosis of sialoglycoconjugated lectin receptor on the tumor cell surface; (iii) the endocytosis of RC-RNase mediated by the receptor; or (iv) the inhibition of protein synthesis leading to cell death (Nitta et al., 1993,1994).

At present, the structure of this protein or its ligand complexes has not been solved. The molecular basis of the catalytic and lectin-receptor binding properties of RC-RNase is also not known, nor are its mechanisms of action. The active-site residues responsible for the substrate recognition for nuclease activity and the sialic acid binding for tumor cells have also not yet been identified. Toward answering some of these questions we have undertaken the task of determining the solution structure of RC-RNase and its ligand complexes using NMR methods. The excellent dispersion in proton NMR spectra and the exceptional stability of RC-RNase allowed us to assign over 95% of the backbone and the majority of the side-chain protons by analyzing a large set of 2D ^{1}H NMR spectra obtained at several temperatures and pH conditions without isotopically labeled protein. In this paper we describe NMR resonance assignments and the secondary structure identification of RC-RNase. Studies on the RC-RNase interaction with substrate analogs such as cytidylyl-(2'-5')-guanosine, 2'-deoxycytidylyl (3'-5')-2'-deoxylguanosine, sialic acid and other trisaccharides are in progress in our laboratory. A direct comparison of the current results with those obtained from RC-RNase/ligand complexes would help to identify the residues at the interaction sites, and to provide insights into macromolecular recognition.

Sequence analysis has shown that RC-RNase/SBL-C is a 111-amino acid protein whose sequence is highly homologous to that of an RNase isolated from the liver of *Rana catesbeiana* (Titani et al., 1987; Nitta et al., 1989), and also relatively similar to those of human angiogenin (Kurachi et al., 1985), onconase (P-30 protein) isolated from *R. pipiens* eggs (Mikulski et al., 1990; Ardelt et al., 1991), and bovine pancreatic RNase A (Potts et al., 1962; Smyth et al., 1963). Thus, this protein belongs to the superfamily of pyrimidine-base-specific RNases (Nitta et al., 1993,1994). However, there are substantial differences among these proteins. For example, both RC-RNase and P-30 are lectins and are capable of inhibiting tumor cell growth. On the other hand, RNase A from bovine pancreas and angiogenin are not lectins and possess no antitumor or antiviral activity. In fact, Youle et al. (1994) demonstrated that the P-30 protein 'inhibited immunodeficiency virus type 1 replication in H9 leukemia cells 90–99% over a 4-day incubation at a concentration nontoxic to uninfected H9 cells', while 'bovine pancreatic RNase A has no detectable antiviral activity, demonstrating a striking selective antiviral activity among homologous ribonucleases'. Thus, the results obtained from the present study will not only shed light on understanding the molecular mechanism of this superfamily of ribonucleases, but can also provide insight into the specific lectin and antitumor activities of RC-RNase and P-30.

Materials and Methods

Preparation of RC-RNase

Extraction and purification of RC-RNase from bullfrog oocytes were accomplished following the procedures described previously (Liao et al., 1996), and all operations were carried out at 277 K. Briefly, the oocytes were released from the ovaries (cut into approximately 4-cm^3 pieces) by incubation with 0.15% (w/v) type-II collagenase. The ribonuclease was purified by precipitation of yolk granules, extraction of RC-RNase with 0.09 M NaCl, and selective removal of impurities by chromatograph on phosphocellulose and carboxymethyl cellulose columns. From 100 g of ovary tissue removed from a mature female bullfrog (600 g in weight), 150 mg of RC-RNase could be purified. The ribonuclease activity was assayed by the dinucleotide method (Liao, 1992).

Protein sequence analysis

The purified RC-RNase was reduced with DTT and S-carboxymethylated with iodoacetate (Allen, 1989). The modified protein was cleaved at room temperature with cyanogen bromide in 70% formic acid. The digested products were diluted with water and dried in vacuo on a SpeedVac several times to remove residual acid and by-products. The protein was also digested by protease Lys C (100:1, w/w) at 298 K overnight. The acid-free digests and the protease-digested products were separated by reverse-phase HPLC on a C_{18} column (4.6 mm × 25 mm, Vydac, Hesperia, CA, U.S.A.) using a Waters automated gradient controller. The column was first equilibrated with 0.1% trifluoroacetic acid (TFA) and then eluted with a linear gradient of 15 to 50% acetonitrile containing 0.06% TFA. The flow rate was 0.6 ml/min. The separated peptides were collected and dried on a SpeedVac for sequence analyses. Automated cycles of Edman degradation were performed on an Applied Biosystem Inc. gas/liquid-phase Model 470A/900A sequencer, equipped with an on-line Model 120A phenylthiohydantoin amino acid analyzer (Hewick et al., 1981). While the first eight residues were not sequenced due to the formation of N-terminal pyroglutamates, the remaining C-terminal 103 amino acids were; these results, together with the partial sequence of RC-RNase previously reported (Liao, 1992), provide the complete sequence of the protein, and they are in total agreement with the sequence determined for SBL-C (Titani et al., 1987).

Mass spectrometry

The mass spectrometry analyses of RC-RNase were performed on a VG Quatto-Bio-Q (Fisons Instruments, UG Biotech, Altrincham, U.K.), a triple-quadrupole in-

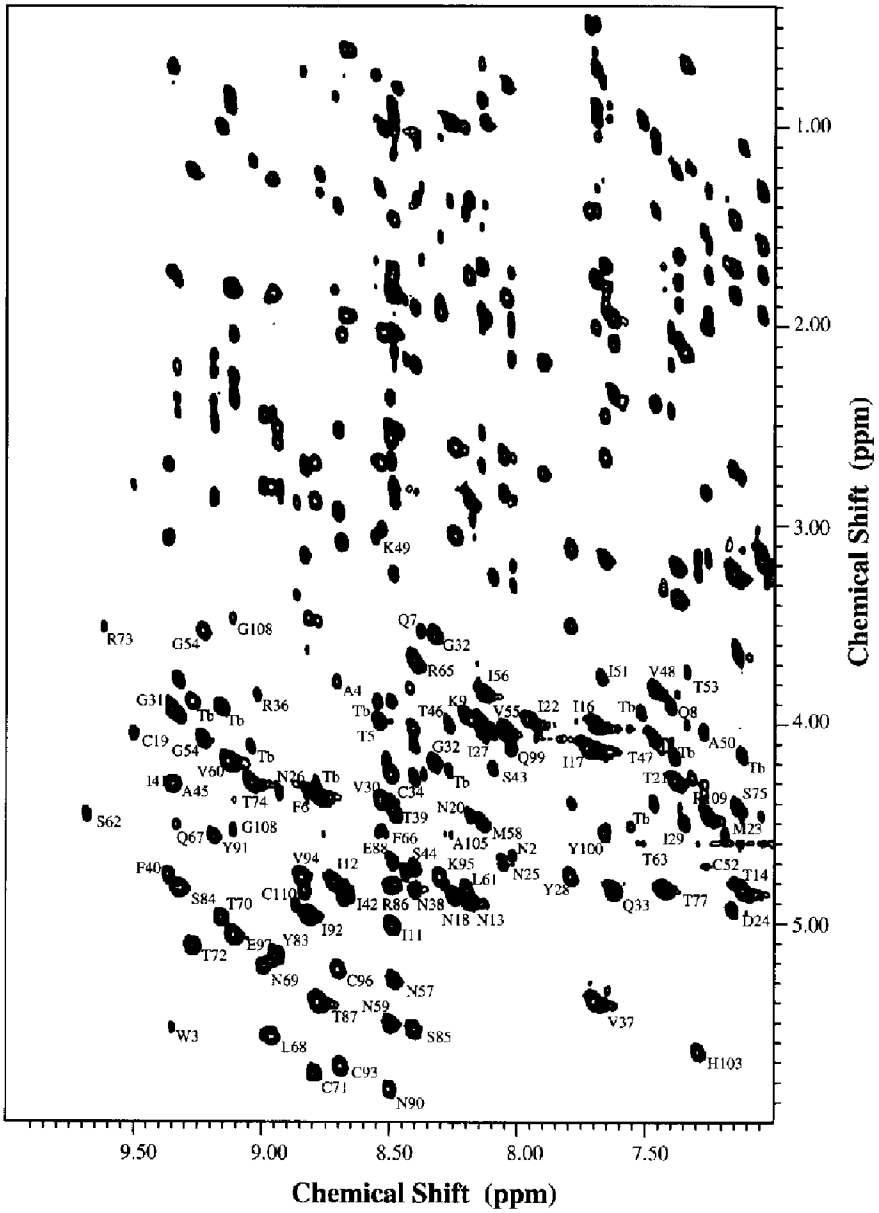

Fig. 1. Fingerprint region from a representative 2D TOCSY spectrum of a 2 mM RC-RNase sample in 50 mM phosphate, 10% v/v D_2O at pH 3.5. The spectrum was acquired at 310 K with an MLEV-17 spin-lock time of 55 ms, using 2048 complex data points along the F2 dimension and 700 t_1 increments.

strument with a mass range for singly charged ions of 4000. Samples were introduced and monitored as described previously (Hong et al., 1994). The molecular weight determined by mass spectrometry is identical to that calculated from the amino acid sequence of RC-RNase.

NMR spectroscopy

Samples for NMR experiments contained about 0.3 ml of 2–3 mM protein in 50 mM phosphate buffer, at pH 3.5–7.0. Buffer exchange and pH adjustments were achieved by repeated dilution with appropriate buffers and concentrating with centricon filters. The pH of the final filtrate was taken as the pH of the protein sample. Upon attaining the desired pH, 10% (v/v) of D_2O was added. For preparing the sample in D_2O, the concentrated protein sample was repeatedly lyophilized and redissolved in D_2O. The pH values were measured with a JENCO microelectronic pH-vision model 6071 pH meter equipped with a 4-mm electrode. All reported pH values were direct readings from the pH meter without correction for isotope effect. For monitoring the exchange rates of labile protons, the concentrated sample in H_2O was lyophilized only once and redissolved in D_2O (99.99% deuterium) and NMR spectra were acquired immediately and subsequently at appropriate time intervals. Sodium 3-trimethylsilylpropionate-2,2,3,3-d_4 (TSP) was used as an internal chemical shift standard.

All NMR spectra were recorded at 600.13 MHz on a

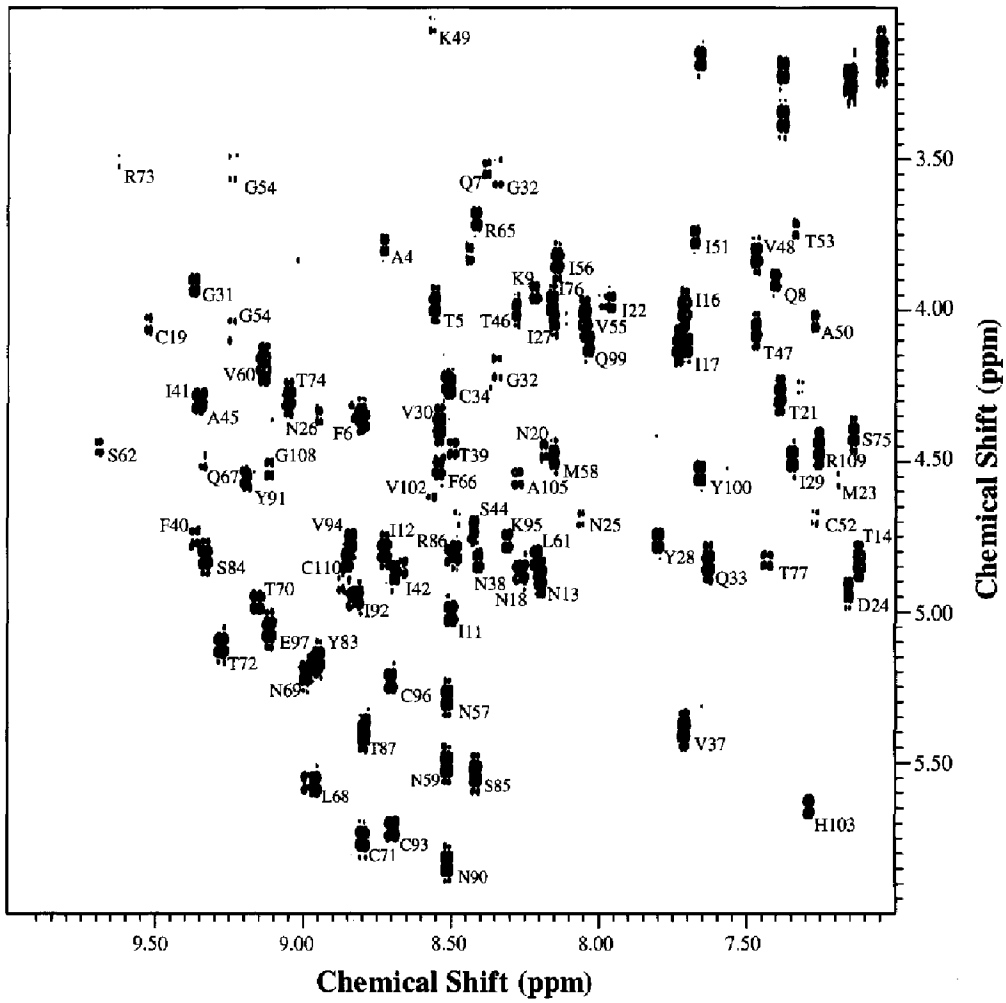

Fig. 2. The fingerprint region of a DQF-COSY spectrum of RC-RNase acquired at 310 K, using 4000 complex data points and 1024 t_1 increments. Sample conditions were the same as in Fig. 1. All the H^N–H^α cross peaks were assigned, and are labeled in the figure.

Bruker AMX-600 spectrometer (Bruker, Karlsruhe, Germany). For DQF-COSY spectra, 700 to 1024 t_1 increments were collected, each with 16 to 32 scans of 2K or 4K complex data points (Rance et al., 1983). The TOCSY spectra were collected with 512–700 t_1 increments with 16 transients of 2K complex points (Bothner-By et al., 1984; Bax and Davis, 1985). We used MLEV-17 spin-lock sequences of 18 and 55 ms in D_2O media and 18, 32, 45 and 55 ms for protic media. For the NOESY spectra, 512–700 t_1 increments were collected, each with 32 scans of 2K complex data points (Kumar et al., 1980; Bodenhausen et al., 1984). Mixing times of 50, 100 and 200 ms were used. Spectra were recorded in time-proportional phase-incrementation (TPPI) mode (Redfield and Kunz, 1975; Drobny et al., 1979; Marion and Wüthrich, 1983). Water suppression was achieved by 1.4 s presaturation at the water frequency, or by the gradient method (Piotto et al., 1992). All spectra were collected with 8196 Hz spectral widths.

The data were transferred to an SGI personal IRIS or an SGI INDIGO workstation (Silicon Graphics, Mountain View, CA, U.S.A.) for all processing and further analysis using Bruker UXNMR and AURELIA software packages. All data sets acquired were zero-filled to equal amounts of points in both dimensions prior to further processing. A 60°-shifted skewed sine-bell window function was used in all NOESY and TOCSY spectra and a 20°- or 30°-shifted skewed sine-bell function was used for all COSY spectra. To help resolve spectral overlap, data were collected at temperatures of 298, 300, 305, 310 and 320 K for the pH 3.5 sample in protic media, at 300, 305, 310 and 320 K for the pH 7.0 sample in protic media, at 300, 305 and 310 K for the pH 3.5 sample in D_2O, and at 305 and 320 K for the pH 7.0 sample in D_2O.

Results

Resonance assignments

RC-RNase is a well-behaved protein with excellent stability over a wide range of pH values (between 3.5 and 9.0) and temperatures (up to 335 K). RC-RNase showed excellent chemical shift dispersion in its proton NMR spectra. Thus, even for a protein of this size, we were able

to assign the backbone proton resonances for all but five of the residues, by analysis of a large set of 2D NMR spectra recorded at several pH values (between 3.5 and 7.0) and temperatures (between 298 and 320 K). The best spectra were those obtained at 310 K and pH 3.5, where the amide proton exchange is the slowest. The protein is still active at this low pH (Liao, 1992). Therefore, all the spectra shown in this paper and all chemical shift values reported in Table 1 are those obtained at 310 K and pH 3.5 in the presence of 50 mM phosphate buffer, unless specified otherwise. Figure 1 shows the fingerprint region of a representative TOCSY spectrum of a 2.0-mM RC-RNase sample, recorded with a 55-ms mixing time. A corresponding DQF-COSY spectrum, showing 96 of the maximally 104 expected H^N–H^α cross peaks is shown in Fig. 2. The excellent dispersion and efficiency of magnetization transfer are evident. Most of the spin systems were identified from these spectra.

Aromatic residues

The assignment of the spin systems of the aromatic rings in phenylalanines, tyrosines, and tryptophan was obtained from a set of COSY, TOCSY and NOESY spectra in which resonances for all the aromatic protons were identified. All four tyrosines (at positions 28, 83, 91 and 100) and all four phenylalanines (at positions 6, 40, 66 and 104) are fully assigned. Initially, we had difficulties in assigning the aromatic proton resonances of Tyr^{83} due to the presence of four resonances and of Phe^{66} due to resonance overlapping. Final assignments, however, were made only after sequential assignments were completed. We believe the four ring proton resonances for Tyr^{83} are due to the presence of two conformations. However, we cannot rule out the possibility that they are due to the four ring protons being in a rigid and magnetically asymmetric environment. The connectivities between the aromatic rings and the aliphatic protons of all tyrosines and phenylalanines were established from their respective H^β–H^δ NOE cross peaks. Trp^3 is a unique residue and its proton resonances have been fully assigned. The characteristic $H^{\delta 1}$–$H^{\varepsilon 1}$ COSY cross peak of tryptophan was readily identified. The connectivities between benzene and indole rings of tryptophan were obtained from the NOE cross peak between $H^{\zeta 2}$–$H^{\varepsilon 1}$. The identification of its amide proton was based on a NOE connectivity observed between this proton and H^δ in the indole ring, and was further confirmed in sequential assignment. Two sets of COSY and TOCSY cross peaks between $H^{\delta 2}$ and $H^{\varepsilon 1}$ in the imidazole ring of histidines were observed; their characteristic shifts at different pH values also confirmed these assignments. For His^{103}, the connectivity between the imidazole ring and the main chain was obtained from the NOE cross peak between $H^{\delta 2}$–H^β protons. The other protons were identified from their connectivities to H^β protons in TOCSY spectra. No NOE cross peak was observed between the imidazole ring protons and the aliphatic protons of His^{10}. By exclusion, the remaining set of $H^{\delta 2}$–$H^{\varepsilon 1}$ COSY cross peaks was assigned to His^{10}. The H^α, H^β and amide proton of His^{10} were identified in the sequential assignment.

Aliphatic residues

Ala^4, Ala^{45} and Ala^{50} proton resonances were assigned from their characteristic cross peaks between H^α and H^β methyl protons. The amide and α-proton resonances of Ala^{45} overlapped with those of Ile^{41} at 310 K, but these two resonances were resolved at 298 K. The slowly exchanging amide proton of Ala^{105} was readily observed in D_2O spectra, and it allowed us to establish connectivities to its H^α, which was otherwise buried under the water peak in spectra obtained in protic media, and to its methyl resonances as well. Five of the valines (at positions 30, 37, 48, 55 and 60) were identified from the characteristic TOCSY network formed by its H^α, H^β and H^γ-methyl resonances. The intensities of the TOCSY H^N–H^β and H^N–H^γ cross peaks for Val^{94} were very low, and their identities were further confirmed in sequential assignment. The H^α of Val^{102} is very close to the water resonance, and its H^α–H^N cross peak was revealed in the COSY and TOCSY spectra obtained in D_2O. Assignments of leucines and isoleucines were difficult. We identified a fewer number of spin networks typical of leucines and isoleucines than expected from the protein sequence. Analyses of the aliphatic region in the COSY and TOCSY spectra were not helpful in assigning these residues. The identification of Leu^{61} was achieved in the sequential assignment process. Two sets of closely spaced resonances were observed for Leu^{68}. Increasing the temperature to 320 K resulted in better resolution of the H^N resonances in the two conformers. For each of the two Leu^{68} conformers, only one of the two H^δ-methyl peaks was observed in their TOCSY spin networks, and NOESY connectivities were employed to identify the other methyl proton resonances. There are 14 isoleucine residues, at positions 11, 12, 16, 17, 22, 27, 29, 41, 42, 51, 56, 76, 92 and 107. The assignments of isoleucines were mainly accomplished in the sequential assignment process.

Small residues

Two glycines at positions 32 and 54 were fully assigned based on their characteristic COSY cross peaks. The H^α protons of Gly^{31} were degenerate at 310 K and were identified at 298 K. The other two glycines at positions 106 and 108 have only one H^N–H^α COSY cross peak each and were identified from TOCSY spectra. Their assignments were reconfirmed in the sequential assignment. The 13 threonine residues at positions 5, 14, 21, 39, 46, 47, 53, 63, 70, 72, 74, 87 and 89 were all fully assigned. The other two threonines at positions 64 and 77 were assigned based on NOE sequential assignments. Two sets of H^α,

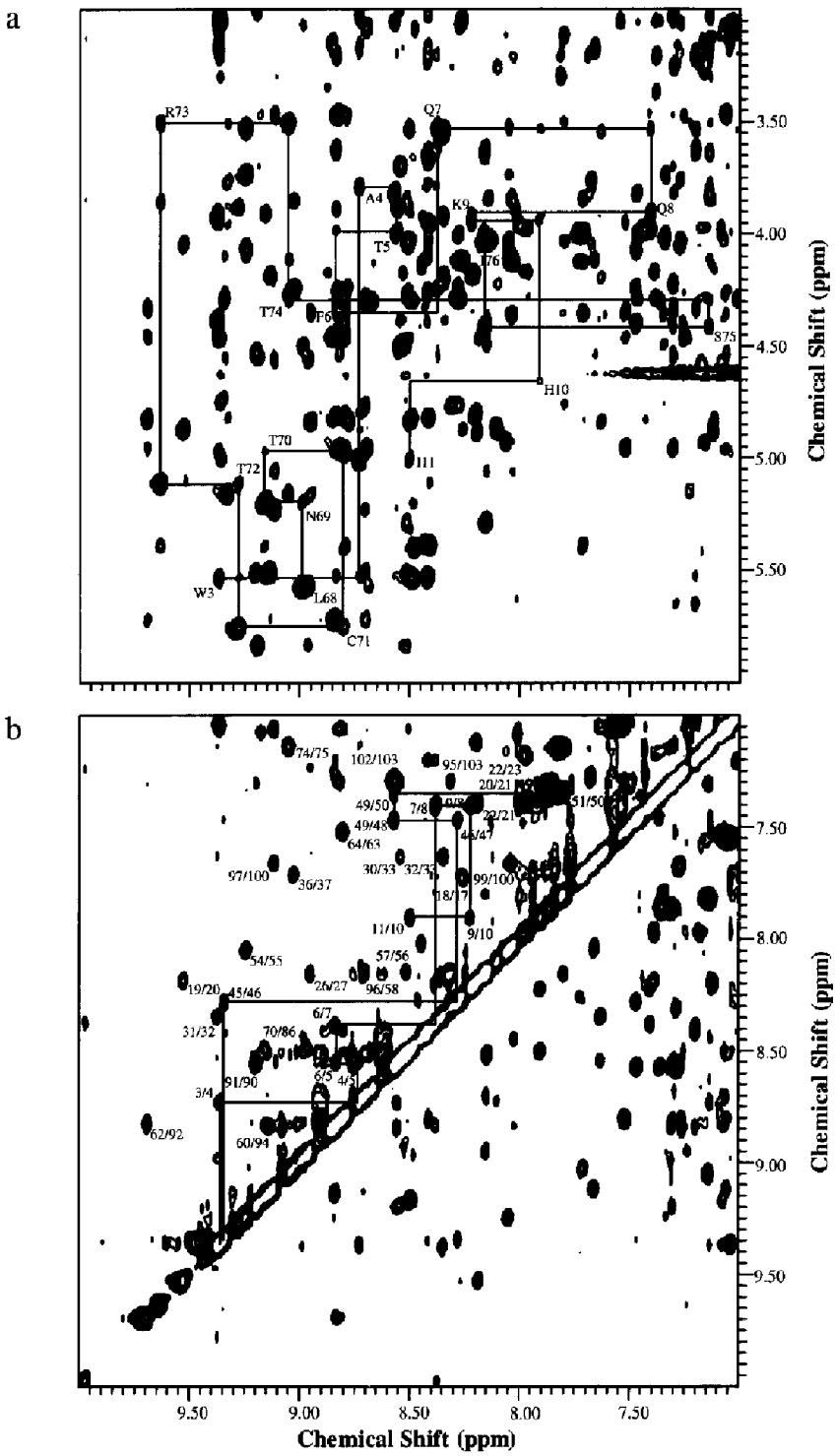

Fig. 3. (a) The fingerprint region of a NOESY spectrum (mixing time 100 ms) of RC-RNase acquired at 310 K. Sample conditions were the same as in Fig. 1. Sequential connectivities from Leu^{68} to Ile^{76} and from Trp^{3} to Ile^{11} are shown. (b) The H^N–H^N region of a NOESY spectrum (mixing time 100 ms) of RC-RNase acquired at 310 K. Sample conditions were the same as in Fig. 1. Sequential H^N–H^N connectivities from Trp^{3} to Ile^{11} and from Ala^{45} to Ile^{51} are shown.

H^β and amide proton resonances were observed for Thr^{87} even at temperatures as high as 320 K. There are 27 non-aromatic residues with AMX spin systems, and their spin systems were all identified from COSY and TOCSY spectra. The H^N, H^α, H^β and side-chain amide proton resonances of all 12 asparagines (at positions 2, 13, 18, 20, 25, 26, 38, 57, 59, 69, 90 and 98) have been identified. Asp^{24} was identified from sequential assignment. Except for Cys^{81}, which is flanked by prolines, all other seven cysteine residues (at positions 19, 34, 52, 71, 93, 96 and 110)

were fully assigned. Cys[81] was assigned by way of exclusion. Five serines (at positions 43, 44, 75, 84 and 85) were assigned based on their characteristic β-proton chemical shifts. The two β-protons of Ser[62] could not be assigned from the COSY and TOCSY spectra and were eventually assigned in the sequential assignment stage. The identification of the hydroxyl group of Ser[62] at 6.13 ppm was based on a TOCSY cross peak with its H^{β} protons and a NOESY cross peak with its H^{α} and H^{β} protons.

Long-chain residues

Full assignment was obtained for Glu[88] and Glu[97]. The spin network of Glu[97] was easily identified, while the assignment of Glu[88] was made during sequential assignment. Only the α-proton of the N-terminal pyroglutamate (PE-1) has been assigned. The H^{N}, H^{α}, H^{β} and H^{γ} resonances of all five glutamines (at positions 7, 8, 33, 67 and 99) were assigned from their AM(PT)X spin systems. Their side-chain amide proton resonances, with the exception of

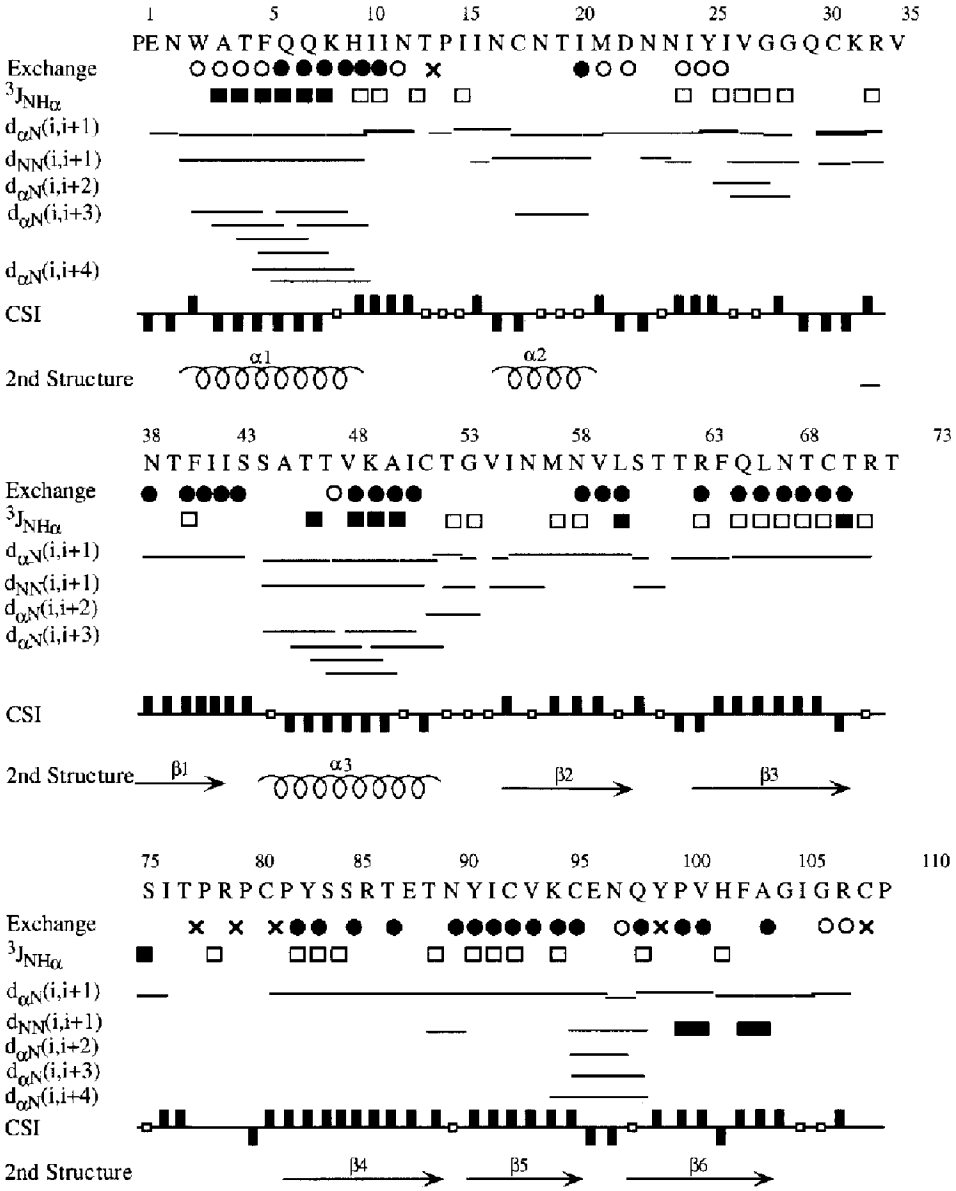

Fig. 4. Sequence of RC-RNase, the amide proton exchange rates, $^3J_{NH\alpha}$, summary of the sequential and medium-range NOEs involving H^{N} and H^{α} protons, chemical shift index and the deduced secondary structures of RC-RNase. Amide protons that remained observable in the TOCSY spectrum after 24 h are labeled with filled circles (slow-exchange protons), those that were observable after 5 h in D_2O at 310 K and pH 3.5 are marked with open circles (medium-exchange protons), and those that were not observable upon addition of D_2O (fast-exchange protons) are not marked. Open squares represent $^3J_{NH\alpha} > 8$ Hz and filled squares represent $^3J_{NH\alpha} < 6$ Hz. The chemical shift index (CSI) displays the chemical shift differences between the observed C^{α} proton chemical shift of a particular residue and the expected random-coil C^{α} proton chemical shift of the same amino acid. Positive bars in CSI indicate downfield shifts of more than 0.1 ppm, while upfield shifts of more than 0.1 ppm are indicated by negative bars. Open squares in CSI indicate that the C^{α} proton chemical shifts are within ±0.1 ppm of those expected from random-coil values. The NOE intensities are indicated by the thickness of the black bars, with thicker bars representing stronger NOEs.

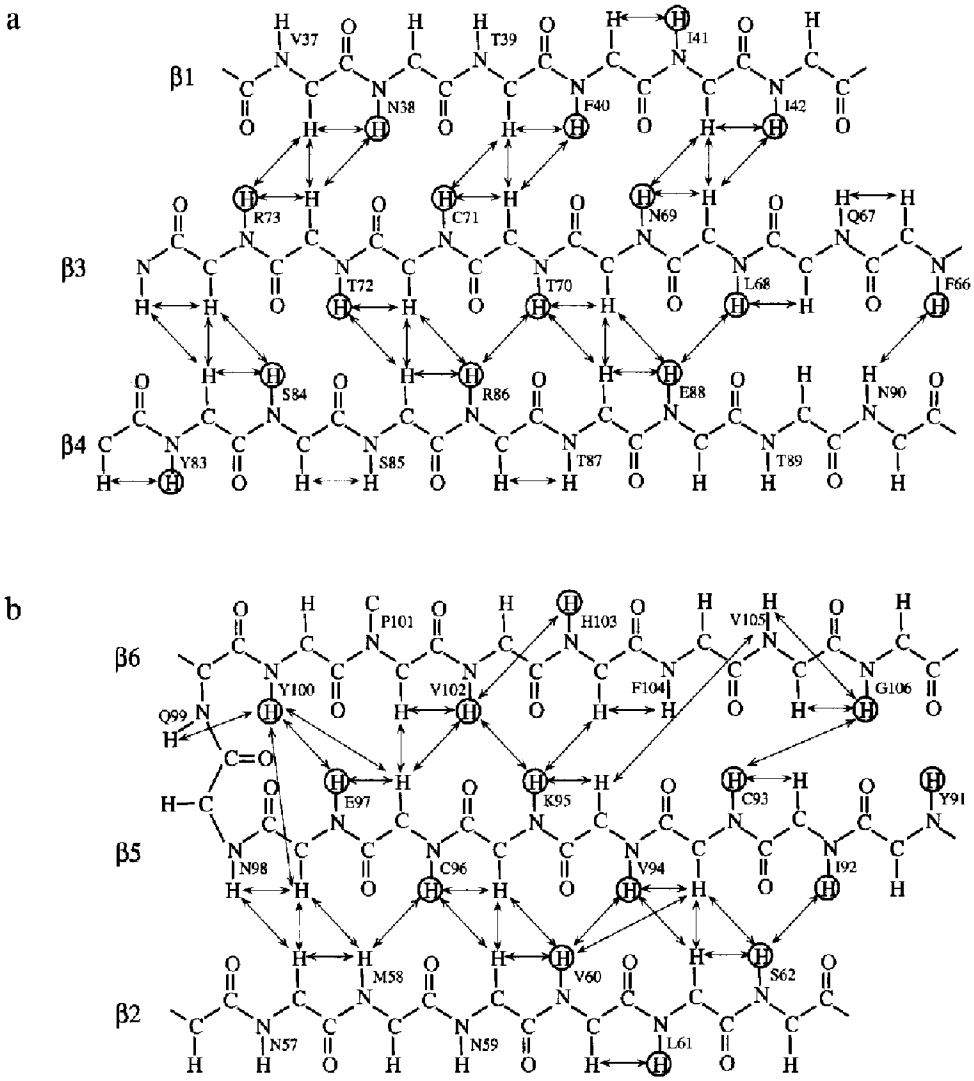

Fig. 5. The proton NOE networks of two triple-stranded, antiparallel β-sheets of RC-RNase. NOEs are indicated by arrows. (a) Sheet a; (b) sheet b. The amide protons with very slow exchange rates are circled.

Gln[7], were also assigned. Two sets of resonances were observed for Gln[67]; increasing the temperature to 320 K resulted in the disappearance of both amide protons. All proton resonances of both Met[23] and Met[58] have been assigned. The H^N, H^α, H^β, H^γ, and H^δ resonances of four arginine residues at positions 36, 65, 86 and 109 have been assigned. Only partial assignment of Arg[73] was accomplished, while assignment of Arg[79] remains elusive. The COSY H^δ–H^ε cross peaks of all arginines have been assigned to their corresponding residues. There are four lysines, at positions 9, 35, 49 and 95. The H^N and all non-exchangeable side-chain resonances of Lys[49] were identified readily from its TOCSY cross peaks. The assignment of the remaining three lysines was accomplished in the sequential assignment. The assignments of proline (at positions 15, 78, 80, 82, 101 and 111) have been difficult due to resonance overlapping. Only three $d_{\alpha\delta}(i,i+1)$ connectivities in the NOESY spectra obtained in D_2O could be identified. These were subsequently assigned to Pro[15], Pro[82] and Pro[101] in the sequential assignment process. The assignment of the other three prolines remains elusive.

Sequential resonance assignments

The standard strategy for sequential resonance assignments by connecting the intraresidue peaks in the fingerprint or H^N–H^N regions via NOEs from the α-proton to the amide proton or the amide proton to the amide proton of the following residue was employed (Wüthrich, 1986). Our sequential assignment was based mainly on the analyses of NOESY spectra (100 ms mixing time) of RC-RNase dissolved in D_2O and in H_2O at pH 3.5. The general approach was to first analyze the most intense cross peaks in the fingerprint region (Fig. 3a) and the H^N–H^N region (Fig. 3b). The results are summarized in Fig. 4. From the $H^\alpha(i)$–$H^N(i+1)$ and $H^N(i)$–$H^N(i+1)$ cross peaks in the NOESY spectra we made sequential assignments of the following segments: PE-1 to Thr[14]; Pro[15] to Thr[64]; Arg[65] to Ile[77]; and Pro[82] to Cys[110].

Secondary structure identification

The secondary structures of RC-RNase were identified by the detection of specific patterns of short-, medium- and long-range NOEs (Wüthrich, 1986). The α-proton chemical shifts (Pastore and Saudek, 1990; Wishart et al., 1991,1992), hydrogen-exchange rates of amide protons and the three-bond H^N-H^α coupling, $^3J_{HN\alpha}$, were employed to further confirm the existence of a specific secondary structure. Figure 4 shows the specific NOE connectivities, $^3J_{HN\alpha}$, and amide proton exchange rates of backbone protons. From this figure we identified the presence of three α-helices and six β-strands. The first α-helix (helix α1) starts at residue Trp^3 and ends at Ile^{11}. This helix is well defined with medium $d_{\alpha N}(i,i+3)$ and $d_{NN}(i,i+1)$ and small $d_{\alpha N}(i,i+4)$ NOEs, and medium amide proton exchange rates (observable after 5 h) for Trp^3 to Phe^6, and slow exchange rates (observable after 24 h) for Gln^7 to Ile^{11}. The unusual H^α chemical shift observed for Trp^3 can be explained by the ring-current effects arising from the neighboring aromatic rings of Phe^6 and Tyr^{100}, whose presence is indicated by their long-range NOE peaks to Trp^3. The small three-bond J-coupling observed for this segment is consistent with the formation of an α-helix. The second α-helix (helix α2) extends from Asn^{18} to Met^{23}. Weak $d_{\alpha N}(i,i+1)$ and strong $d_{NN}(i,i+1)$ NOEs were observed in this region. However, this helix is less stable, as typified by the weaker $d_{\alpha N}(i,i+3)$ NOEs, faster amide proton exchange rates, except for Met^{23}, and intermediate $^3J_{NH\alpha}$. The third α-helix (helix α3), extending from Ala^{45} to Thr^{53}, is also well defined with strong $d_{\alpha N}(i,i+3)$ and $d_{NN}(i,i+1)$ NOEs, medium amide proton exchange rates for residues Val^{48} and Lys^{49} and slow amide proton exchange rates for residues Ala^{50} to Cys^{52}. The chemical shift index and $^3J_{NH\alpha}$ are also in good agreement with this segment being in an α-helical conformation.

The dominant feature of the secondary structure of RC-RNase is the presence of two triple-stranded, antiparallel β-sheets. Extensive inter- and intrachain NOE cross peaks characteristic of β-sheet structures were observed (Fig. 5). The first β-sheet (sheet a) includes the following three strands: Val^{37} to Ile^{42} (β1-strand); Phe^{66} to Arg^{73} (β3-strand); and Tyr^{83} to Ile^{90} (β4-strand), with β3 forming the central strand. The second β-sheet (sheet b) is made up of the following strands: Asn^{57} to Ser^{62} (β2-strand); Ile^{92} to Glu^{97} (β5-strand); and Tyr^{100} to Gly^{106} (β6-strand), with β5 forming the central strand. The unusual high-field shift of the α-proton of Arg^{73} in strand 3 is probably due to the ring-current effect of Tyr^{83} in strand 4. The NOE pattern between strands 5 and 6 is unusual, suggesting that sheet b is a distorted β-sheet structure. Part of the reason for the distortion is probably the presence of the turn at Glu^{97} and Tyr^{100}.

There are a total of 48 residues which do not form part of the α-helix or β-strand structure. Most of these residues are clustered in three large loop regions, loop 1 (Ile^{12} to Asn^{18}), loop 2 (Asp^{24} to Arg^{36}), and loop 3 (Thr^{74} to Pro^{82}). We did not observe specific NOEs which can be employed to define the secondary structure of the following residues: Ile^{12} to Asn^{18} (loop 1), Asp^{24} to Arg^{29} (loop 2), Thr^{74} to Thr^{77} (loop 3). All of these residues, except Ile^{12}, have medium or fast amide proton exchange rates. Thus, these residues do not have a defined conformation and might be located on the protein surface. The NOE pattern, amide proton exchange rates, and $^3J_{NH\alpha}$ for residues in the three regions, Val^{30} to Gln^{33}, Thr^{53} to Ile^{56}, and Glu^{97} to Tyr^{100} are consistent with these residues being in β-turn structures. Furthermore, the observation of $d_{\alpha N}(97,99)$, $d_{\alpha N}(97,100)$ and $d_{NN}(97,100)$ suggests that residues Glu^{97} to Tyr^{100} form a type I β-turn. Long-range NOEs between this turn and residues Ile^{56} and Met^{58} were observed. The structure of the region between Pro^{78} and Pro^{82} is still uncertain due to the presence of three not fully assigned proline residues. Tyr^{91}, which connects β4 and β5, appears to form a β-bulge. Only sequential and intraresidue NOEs were observed for the terminal residues, PE-1, Asn^2, and Ile^{107} to Pro^{111}. Presumably these residues are mobile and undefined.

Discussion

Structural comparison among different RNases

RC-RNase belongs to the pancreatic ribonuclease superfamily. It shares 27% sequence identity to the mammalian bovine pancreatic RNase A and 53% sequence identity to an amphibian ribonuclease, the P-30 protein. However, in addition to possessing ribonucleolytic activity, RC-RNase is also a lectin and is cytotoxic, similar to P-30 protein (Ardelt et al., 1991; Wu et al., 1993; Liao et al., 1996). In contrast, no cytotoxicity or lectin activity was found for either bovine pancreatic RNase A or angiogenin. The structural basis of the functional differences among these proteins is not known. Therefore, it is interesting to compare the structural differences of these proteins. Figure 6 shows a secondary structure comparison among the four RNases. These four ribonucleases are comparable in molecular size; only angiogenin has three disulfide bonds, compared to four in the other three ribonucleases. All possess three α-helices of similar length, and are located in similar positions. Our NMR data indicate that the α2 helix in RC-RNase is less stable than the corresponding helices in the other RNases. Both RNase A (Rico et al., 1991; Santoro et al., 1993) and angiogenin (Reisdorf et al., 1994) have seven β-strands, compared to six observed in P-30 (Mosimann et al., 1994) and RC-RNase. The β-strands in all four ribonucleases form two antiparallel β-sheets. As shown in Fig. 6, the β-strands of all four ribonucleases are similar in length and location, with the exception of the region between Lys^{61} and Ser^{75} (RNase A numbering system), where two β-strands were observed for RNase A and angiogenin, but only one for P-30 and

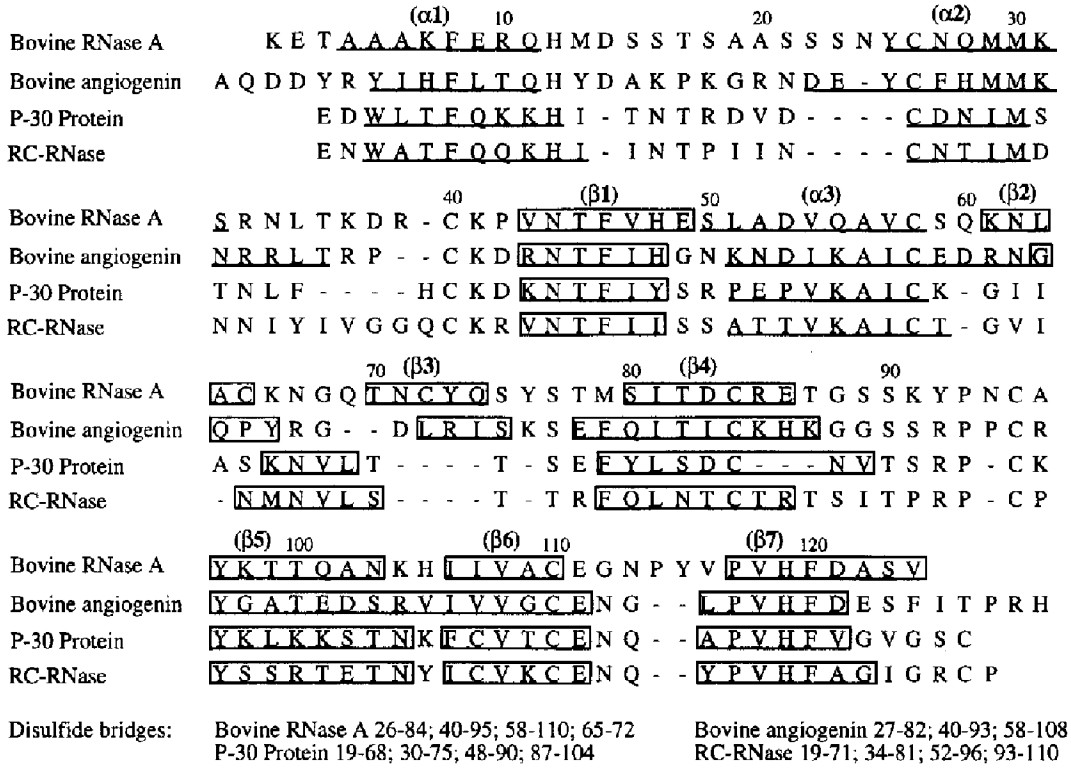

Fig. 6. Secondary structure comparison of four ribonucleases: bovine ribonuclease A, bovine angiogenin, RC-RNase and P-30 protein from *R. pipiens* oocyte. α-Helical structures are underlined and β-strands are boxed. Residues are numbered according to the sequence of bovine RNase A.

RC-RNase. Another unique property of RC-RNase is the presence of nearly equal populations of two conformers, a property not observed in any other RNases. The functional significance of the two conformers has yet to be elucidated.

Structure comparison at pH 3.5 and 7.0

While RC-RNase is stable over wide temperature and pH ranges, the optimal activity of RC-RNase occurs around pH 7.5, and it drops substantially at both lower and higher pHs. Thus, it is interesting to compare the structural differences observed at different pHs. Structural differences can be deduced qualitatively from changes in amide proton exchange rates, from chemical shift changes, and from NOE connectivities. We have obtained two sets of NMR spectra and have assigned most of the proton resonances at both pH 3.5 and 7.0. In comparison, no major changes in NOE connectivities, especially those long-range NOEs characteristic of specific secondary structures, were observed. The overall exchange rates of most NH protons are faster at neutral pH, as expected from the increased intrinsic exchange rate of the amide proton at high pH. Specifically, seven fast-exchanging amide protons located in nonstructured regions (Asn^{2}, Asn^{18}, Cys^{19}, Asn^{26}, Gly^{31}, Arg^{36} and Ala^{45}) observable at pH 3.5 were missing at neutral pH. The slow-exchanging NH protons of Gln^{7}, Gln^{8}, Ala^{50}, Ile^{51}, Arg^{73}, Arg^{86} and Glu^{88} disappeared after 10 h in D_2O at neutral pH. However, the NOE connectivities among these protons are the same as those observed at pH 3.5, suggesting the perseverance of the secondary structures in these regions. Only six NH protons (Val^{60}, Phe^{66}, Leu^{68}, Asn^{69}, Ile^{92} and Val^{94}) located in the β2, β3 and β5 regions were still observable after 24 h in D_2O at pH 7.0, compared to 41 at pH 3.5 (Fig. 4). The corresponding residues of the six slow-exchanging amide protons in P-30 are clustered at the bottom of the bowl-shaped structure. Thus, this region must represent the most protected region.

Most of the α-proton resonances shift less than 0.02 ppm upon changing the pH from 3.5 to 7.0. The four exceptions are Asp^{24} (0.05 ppm), Asn^{57} (0.04 ppm), Glu^{97} (0.04 ppm) and His^{103} (0.2 ppm). All but Asn^{57} have a pK_a value between pH 3 and 7. Asn^{57} is paired to Glu^{97} in forming the β-sheet structure. Therefore, all the unusual α-proton chemical shift changes may be attributed to a charge effect. Furthermore, all residues showing the presence of two conformations at pH 3.5 also exist in two conformers at pH 7.0. From the above observation we conclude that the structure of RC-RNase is very similar at pH 3.5 and 7.0. This is very interesting and we will need to find more detailed structural differences to explain the greatly reduced activity observed at low pH. Apparently, the precise rearrangement of residues around the active site is crucial in determining the enzymatic activity. We are in the process of calculating the detailed three-dimensional structure of RC-RNase.

Multiple conformations

Two amide proton resonances were observed for each of the following 11 residues: Ile^{17}, Ile^{22}, Val^{37}, Ile^{42}, Phe^{66}, Gln^{67}, Leu^{68}, Asn^{69}, Arg^{86}, Thr^{87} and Glu^{88}. We also observed two α-proton resonances for each of the following eight residues: Val^{37}, Ile^{42}, Phe^{66}, Gln^{67}, Leu^{68}, Asn^{69}, Thr^{87} and Glu^{88}. Two resonances were also observed for several side-chain protons of these residues. These residues scattered around loop 1, the α2 helix, the β1 strand, the β3 strand and the β4 strand, suggesting the presence of two conformers in slow exchange for these regions. Figure 7 shows a region of a NOESY spectrum (mixing time 200 ms) obtained at 320 K and pH 7.0, displaying two sets of resonances for Leu^{68}, Asn^{69}, Thr^{87} and Glu^{88}. From the NOE cross-peak intensities we estimated the population ratio of these two conformations to be 40:60 at 320 K. The presence of two chemically different species can be ruled out from the results of mass spectrometry, peptide sequencing and SDS-PAGE gel-electrophoresis, which all showed the presence of only a single protein species. Although the small chemical shift differences between most of the corresponding resonances in the two conformers are too small to allow us to observe the exchange cross peaks near the diagonal, four ring proton resonances at 6.52, 6.60, 6.75 and 7.23 ppm were observed for Tyr^{83}. Six cross peaks among these protons were observed in the TOCSY and NOESY spectra at 310 K in D_2O. Lowering the temperature to 280 K resulted in the observation of only two cross peaks (at (6.52,6.60) and (6.75, 7.23)). On the other hand, at 320 K the cross peaks broadened substantially. When the temperature was raised to 335 K, all the cross peaks disappeared, presumably due to excessive exchange broadening. While it is clear that the observed change with temperature of the cross-peak pattern is due to the kinetic exchange effect, the molecular basis of the exchange process is still not clear. Two possible mechanisms come to mind: (i) the Tyr^{83} ring exists in two conformations and two ring proton resonances are observed for each conformation. Exchange cross peaks can be observed if there is conformational exchange. This observation is consistent with the observed multiple conformation of the nearby residues; (ii) the Tyr^{83} ring exists in only one conformation; however, the two sides of the ring are magnetically asymmetric such that all four ring protons resonate at different frequencies. Slow ring flipping results in the observation of exchange cross peaks. At present we are unable to distinguish between these two possibilities. Thus, we believe that the observation of four ring protons of Tyr^{83} is due to the presence of two conformers, and not to asymmetric magnetic environments or chemically different species.

Interestingly, the NOE connectivity patterns of these two conformers are very similar. For example, a NOE cross peak between H^N of Leu^{68} and H^α of Thr^{89} was observed in one conformation, whilst a corresponding NOE cross peak between H^N of Leu^{68} and H^α of Asn^{90}

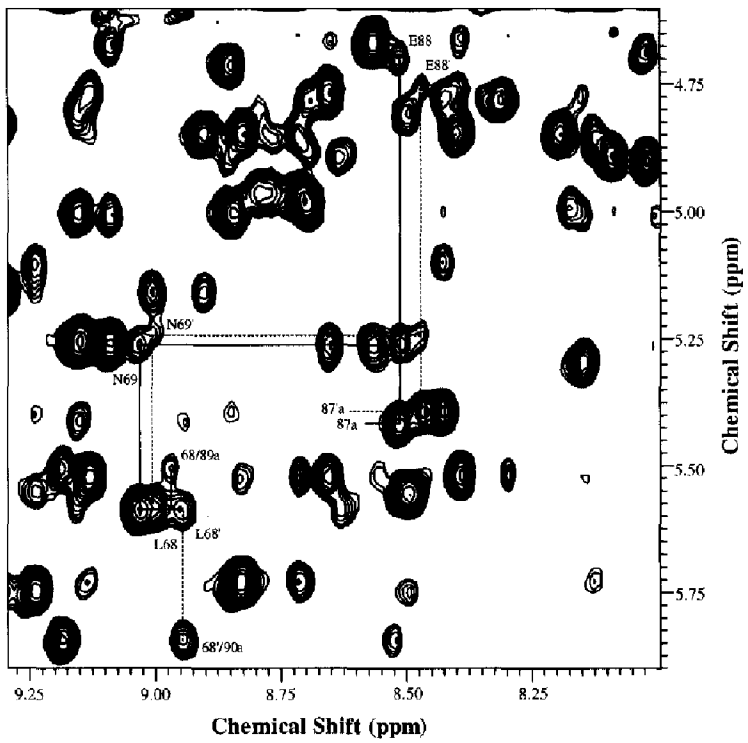

Fig. 7. A selective region of a NOESY spectrum (mixing time 200 ms), showing the presence of multiple conformations of RC-RNase. The spectrum was obtained at 320 K with a 2 mM protein sample in 50 mM phosphate buffer, 90% H_2O/10% D_2O, pH = 7.0.

was observed in the second conformer. Since the chemical shift differences of the corresponding protons in these two conformers are very close, we cannot observe directly exchange cross peaks between them. However, the detailed structural differences and exchange kinetics between these two conformers will be revealed after the final structures have been determined.

Conclusions

Functionally, RC-RNase is very similar to P-30; both possess ribonuclease and lectin activities. Both are also cytotoxic. The secondary structural features deduced from the present study are very similar to those found in the X-ray crystal structure of P-30. Both contain two three-stranded antiparallel β-sheets and three short α-helices. Even more striking are the nearly identical locations of these secondary structures in the two sequences, as shown in Fig. 6. Thus, we expect RC-RNase to adopt a similar bowl-shaped three-dimensional structure as that of P-30. In fact, the preliminary low-resolution structure of RC-RNase, as deduced from limited numbers of NOE constraints, supports our speculation (Chen et al., unpublished observations). Furthermore, addition of cytidylyl-(2'-5')-guanosine, a substrate analog, caused shifts in the proton resonances of several residues (Chen et al., unpublished observations). The corresponding residues in P-30, located at the putative substrate binding cleft, thus further confirmed the structural similarity between these two proteins. We are in the process of calculating the detailed 3D structure of RC-RNase.

Acknowledgements

This work was supported by the National Science Council of the Republic of China, NSC84-2331-B001-041-M08 (T.h.H.), NSC85-2331-B001-058 (T.-h.H.) and NSC 84-2331-B001-022 (Y.D.L.) and the Academia Sinica.

References

Allen, G. (1989) In *Laboratory Techniques in Biochemistry and Molecular Biology*, Vol. 9, 2nd ed. (Eds, Burdon, R.H. and Van Knippenberg, P.H.), Elsevier, Amsterdam, The Netherlands, pp. 19–104.

Ardelt, W., Mikulski, S.M. and Shogen, K. (1991) *J. Biol. Chem.*, **266**, 245–251.

Bax, A. and Davis, D.G. (1985) *J. Magn. Reson.*, **63**, 207–213.

Bodenhausen, G., Kogler, H. and Ernst, R.R. (1984) *J. Magn. Reson.*, **58**, 370–388.

Bothner-By, A.A., Stephens, R.L., Lee, J.T., Warren, C.D. and Jeanloz, R.W. (1984) *J. Am. Chem. Soc.*, **106**, 811–813.

Drobny, G., Pines, A., Sinton, S., Weitekamp, D.P. and Wemmer, D.E. (1979) *Faraday Symp. Chem. Soc.*, **13**, 49–55.

Hewick, R.M., Hunkapiller, M.W., Hood, L.E. and Dreyer, W.J. (1981) *J. Biol. Chem.*, **256**, 7990–7997.

Hong, J.L., Liu, L.F., Wang, L.Y., Tsai, S.P., Hsieh, C.H., Hsiao, C.D. and Tam, M.F. (1994) *Biochem. J.*, **304**, 825–831.

Kawauchi, H., Sakakibara, F. and Watanabe, K. (1975) *Experientia*, **31**, 364–365.

Kumar, A., Ernst, R.R. and Wüthrich, K. (1980) *Biochem. Biophys. Res. Commun.*, **95**, 1–6.

Kurachi, K., Davie, E.W., Strydom, D.J., Riordan, J.F. and Vallee, B.L. (1985) *Biochemistry*, **24**, 5494–5499.

Liao, Y.D. (1992) *Nucleic Acids Res.*, **20**, 1371–1377.

Liao, Y.D. and Wang, J.J. (1994) *Eur. J. Biochem.*, **222**, 215–220.

Liao, Y.D., Huang, H.C., Chan, H.J. and Kuo, S.J. (1996) *Protein Expr. Purif.*, **7**, 194–202.

Marion, D. and Wüthrich, K. (1983) *Biochem. Biophys. Res. Commun.*, **113**, 967–974.

Mikulski, S.M., Ardelt, W., Shogen, K., Bernstein, E.H. and Menduke, H. (1990) *J. Natl. Cancer Inst.*, **82**, 151–153.

Mosimann, S.C., Ardelt, W. and James, M.N.G. (1994) *J. Mol. Biol.*, **236**, 1141–1153.

Nitta, K., Katayama, N., Okabe, Y., Iwama, M., Watanabe, H., Abe, Y., Okazaki, T., Ohgi, K. and Irie, M. (1989) *J. Biochem.*, **106**, 729–735.

Nitta, K., Oyama, F., Oyama, R., Sekiguchi, K., Kawauchi, H., Takayanagi, Y., Hakomori, S. and Titani, K. (1993) *Glycobiology*, **3**, 37–45.

Nitta, K., Ozaki, K., Ishikawa, M., Furusawa, S., Hosono, M., Kawauchi, H., Sasaki, K., Takayanagi, Y., Tsuiki, S. and Hakomori, S. (1994) *Cancer Res.*, **54**, 920–927.

Okabe, Y., Katayama, N., Iwama, M., Watanabe, H., Ohgi, K., Irie, M., Nitta, K., Kawauchi, H., Takayanagi, Y., Oyama, F., Titani, K., Abe, Y., Okazaki, T., Inokuchi, N. and Koyama, T. (1991) *J. Biochem.*, **109**, 786–790.

Pastore, A. and Saudek, V. (1990) *J. Magn. Reson.*, **90**, 165–176.

Piotto, M., Saudek, V. and Sklenar, V. (1992) *J. Biomol. NMR*, **2**, 661–665.

Potts, J.T., Berger, A., Cooke, J. and Anfinsen, C.B. (1962) *J. Biol. Chem.*, **237**, 1851–1855.

Rance, M., Sørensen, O.W., Bodenhausen, G., Wagner, G., Ernst, R.R. and Wüthrich, K. (1983) *Biochem. Biophys. Res. Commun.*, **117**, 479–485.

Redfield, A.G. and Kunz, S.D. (1975) *J. Magn. Reson.*, **19**, 250–254.

Reisdorf, C., Abergel, D., Bontems, F., Lallemand, J.Y., Decottignies, J.P. and Spik, G. (1994) *Eur. J. Biochem.*, **224**, 811–822.

Rico, M., Santoro, J., Gonzalez, C., Bruix, M., Neira, J.L., Nieto, J.L. and Herranz, J. (1991) *J. Biomol. NMR*, **1**, 283–298.

Sakakibara, F., Kawauchi, H., Takayanagi, G. and Ise, H. (1979) *Cancer Res.*, **39**, 1347–1352.

Santoro, J., Gozale, C., Bruix, M., Neira, J.L., Nieto, J.L., Herranz, J. and Rico, M. (1993) *J. Mol. Biol.*, **229**, 722–734.

Smyth, D.G., Stein, W.H. and Moore, S. (1963) *J. Biol. Chem.*, **238**, 227–234.

Titani, K., Takio, K., Kuwada, M., Nitta, K., Sakakibara, F., Kawauchi, H., Takayanagi, G. and Hakomori, S. (1987) *Biochemistry*, **26**, 2189–2194.

Wishart, D.S., Sykes, B.D. and Richards, F.M. (1991) *J. Mol. Biol.*, **222**, 311–333.

Wishart, D.S., Sykes, B.D. and Richards, F.M. (1992) *Biochemistry*, **31**, 1647–1651.

Wu, Y.N., Mikulski, S.M., Ardelt, W., Rybak, S.H. and Youle, R.J. (1993) *J. Biol. Chem.*, **268**, 10686–10693.

Wüthrich, K. (1986) *NMR of Proteins and Nucleic Acids*, Wiley, New York, NY, U.S.A.

Youle, R.J., Wu, Y.N., Mikulski, S.M., Shogen, K., Hamilton, R.S., Newton, D., D'Alessio, G. and Gravell, M. (1994) *Proc. Natl. Acad. Sci. USA*, **91**, 6012–6016.